Neuron
Article

The Control of Semaphorin-1a-Mediated Reverse Signaling by Opposing Pebble and RhoGAPp190 Functions in *Drosophila*

Sangyun Jeong,[1] Katarina Juhaszova,[1] and Alex L. Kolodkin[1,*]
[1]Solomon H. Snyder Department of Neuroscience, Howard Hughes Medical Institute, The Johns Hopkins University School of Medicine, Baltimore, MD 21205, USA
*Correspondence: kolodkin@jhmi.edu
http://dx.doi.org/10.1016/j.neuron.2012.09.018

SUMMARY

Transmembrane semaphorins (Semas) serve evolutionarily conserved guidance roles, and some function as both ligands and receptors. However, the molecular mechanisms underlying the transduction of these signals to the cytoskeleton remain largely unknown. We have identified two direct regulators of Rho family small GTPases, pebble (a Rho guanine nucleotide exchange factor [GEF]) and RhoGAPp190 (a GTPase activating protein [GAP]), that show robust interactions with the cytoplasmic domain of the *Drosophila* Sema-1a protein. Neuronal *pebble* and *RhoGAPp190* are required to control motor axon defasciculation at specific pathway choice points and also for target recognition during *Drosophila* neuromuscular development. Sema-1a-mediated motor axon defasciculation is promoted by *pebble* and inhibited by *RhoGAPp190*. Genetic analyses show that opposing pebble and RhoGAPp190 functions mediate Sema-1a reverse signaling through the regulation of Rho1 activity. Therefore, pebble and RhoGAPp190 transduce transmembrane semaphorin-mediated guidance cue information that regulates the establishment of neuronal connectivity during *Drosophila* development.

INTRODUCTION

Normal nervous system function requires the development of elaborate and precise connections among neurons and their targets. Establishing this complex wiring relies on the combined functions of a large and diverse number of axon guidance molecules that coordinate neuronal process pathfinding and target recognition (Dickson, 2002). During development, neurons extend processes that have at their extending tips highly motile structures called growth cones. Receptors expressed on growth cones recognize multiple cues present in the surrounding extracellular environment and manifest their response through the reorganization of neuronal cytoskeletal components, including actin and microtubules (Dent et al., 2011). Although molecular mechanisms that signal cytoskeletal remodeling have been uncovered for certain classes of guidance cue receptors (Bashaw and Klein, 2010; Kolodkin and Tessier-Lavigne, 2011), we are only just beginning to understand how these signaling pathways are integrated in order to allow for discreet steering of neuronal processes; for many guidance cue receptors little is known about the in vivo signaling events they initiate following ligand engagement.

One major class of extracellular guidance cues is the semaphorin protein family, members of which carry out evolutionarily conserved guidance functions during nervous system development through interactions with receptors that include plexins and various other receptors and coreceptors (Mann et al., 2007). A distinctive feature of these proteins is a conserved semaphorin (Sema) domain and a short plexin-semaphorin-integrin (PSI) domain in their extracellular regions; both of these domains are involved in semaphorin homo-multimerization, which is required for the formation of a ligand-receptor signaling complex (Janssen et al., 2010; Liu et al., 2010; Nogi et al., 2010). Both secreted and transmembrane semaphorins function as ligands to mediate a range of repulsive and attractive guidance functions, however, membrane-bound semaphorins can also mediate bidirectional signaling. For example, the transmembrane semaphorin Sema-1a regulates axon-axon repulsion in *Drosophila* through binding to the plexin A (PlexA) receptor during embryonic development (Winberg et al., 1998; Yu et al., 1998). This canonical "forward signaling" allows semaphorins to act as ligands to activate plexin receptors. More recent work shows that Sema-1a can also participate in "reverse signaling," reminiscent of the well-characterized signaling events involving ephrin-reverse signaling (Egea and Klein, 2007). Sema-1a reverse signaling in *Drosophila* can control neuronal process targeting and synapse formation utilizing PlexA, or unknown ligands, to activate its receptor functions (Cafferty et al., 2006; Godenschwege et al., 2002; Komiyama et al., 2007; Yu et al., 2010). Interestingly, the vertebrate class 6 semaphorin Sema6D regulates cardiac morphogenesis through both forward and reverse signaling (Toyofuku et al., 2004). These observations raise questions relating to how forward and reverse transmembrane semaphorin signaling are coordinated during neural development and also, importantly, how the Sema-1a intracellular domain (ICD) transduces Sema-1a reverse signaling.

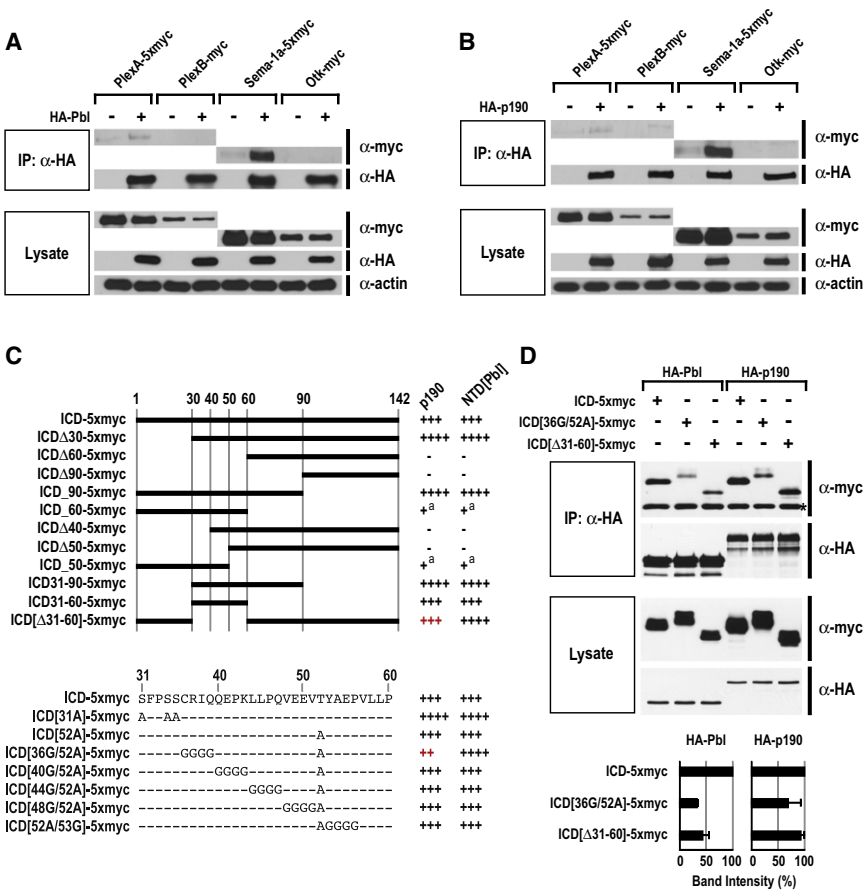

Figure 1. Pebble and RhoGAPp190 Physically Interact with Semaphorin-1a in S2R+ Cells

(A) Interactions between Pbl and PlexA, PlexB, Sema-1a, and Otk in *Drosophila* S2R+ cells. Pbl and p190 were HA-tagged N-terminally, and PlexA, PlexB, Sema-1a and Otk were myc-tagged C-terminally. Pbl was cotransfected with or without PlexA, PlexB, Sema-1a, or Otk. Cell lysates were immunoprecipitated with anti-HA antibody and then blotted with anti-HA or anti-myc antibodies. Input lysates were also blotted with anti-myc, anti-HA, and anti-actin antibodies in the bottom.

(B) Interaction between p190 and PlexA, PlexB, Sema-1a, and Otk in *Drosophila* S2R+ cells. Co-IP experiments were performed as in (A).

(C) Schematic diagram of the Sema-1a ICD constructs used for protein interaction assays with p190 and with the N-terminal domain of Pbl (NTD [Pbl]) (right, a summary of their relative binding abilities). The intracellular domain is 142 amino acids long and numbered at the top. In the right column, the symbols "+" or "−" represent the presence or absence of protein interaction, respectively. The number of + symbols is correlated with relative binding levels. Superscript "a" indicates very weak interactions. At the bottom, amino acids and their mutated sequences within ICD residues 31–60 used for protein interaction assays with p190 and NTD[Pbl] are shown. The "+" sign in red highlights modest but significant differences between p190 and NTD[Pbl].

(D) Binding of wild-type and mutant Sema-1a ICD proteins to full-length Pbl and p190. Asterisk indicates nonspecific IgG bands. Relative binding of Pbl and also p190 to Sema-1a ICD derivatives was measured by averaging band intensities from two experiments, as shown at the bottom. In each column, coimmunoprecipitated wild-type ICD-5xmyc was used as a control (equal to 100% in band intensity). Error bars indicate standard deviation. See also Figure S1.

The Rho family of small GTPases, in combination with their direct regulators (RhoGEFs and RhoGAPs), plays key roles in growth cone steering by mediating localized changes in the actin cytoskeleton (Bashaw and Klein, 2010; Dickson, 2001; Hall and Lalli, 2010; Luo, 2000). Rho GTPases are activated by guanine nucleotide exchange factors (GEFs) that facilitate the exchange of bound GDP with GTP, and they are inactivated by GTPase activating proteins (GAPs) that mediate dephosphorylation of bound GTP to produce GDP. The cycling of Rho GTPases between active and inactive states can, therefore, be regulated by antagonistic relationships between RhoGEFs and RhoGAPs. The activation of Rho GTPases can be regulated spatially through the control of RhoGEF and RhoGAP subcellular localization, and this is influenced by activation of guidance cue receptors that in turn associate directly with GEFs or GAPs (Bashaw and Klein, 2010; Symons and Settleman, 2000). Extracellular cues can also activate signaling pathways that modulate GEF or GAP activity, including phosphorylation or protein-protein interactions that relieve auto-inhibitory intramolecular interactions (Schmidt and Hall, 2002; Shen and Cowan, 2010). Finally, Rho proteins and their regulators have been implicated in mediating repulsive guidance signaling (Derijck et al., 2010; Govek et al., 2005; Hall and Lalli, 2010).

Links between Rho GTPase signaling and Sema-plexin-mediated guidance prompted us to examine interactions between *Drosophila* RhoGEFs, RhoGAPs, and receptor-type guidance molecules. We identified pebble (Pbl), a RhoGEF for Rho1, and RhoGAPp190 (p190), a RhoGAP for Rho1, as signaling molecules with the potential to function downstream of Sema-1a reverse signaling in neurons. Our genetic analyses suggest that Pbl and p190 play key opposing roles in Sema-1a reverse signaling.

RESULTS

Pebble and RhoGAPp190 Bind to Semaphorin-1a

To investigate links between Rho GTPase regulators and semaphorin/plexin-mediated neuronal guidance, we screened several RhoGEF and RhoGAP proteins for their ability to interact with *Drosophila* PlexA, PlexB, and Sema-1a in *Drosophila* S2R+ cells in vitro. We found that Pbl weakly interacts with PlexA, while p190

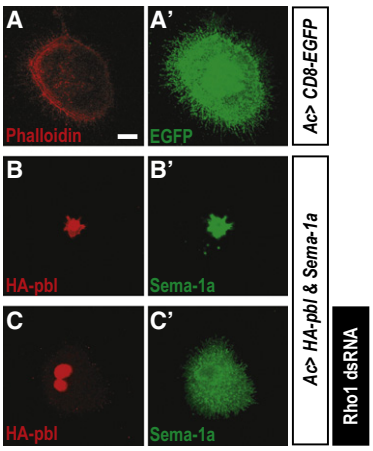

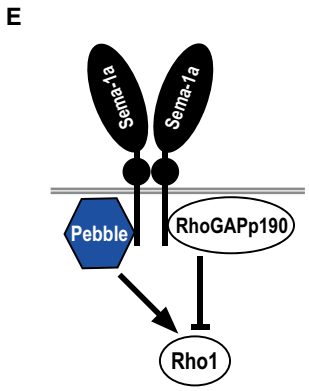

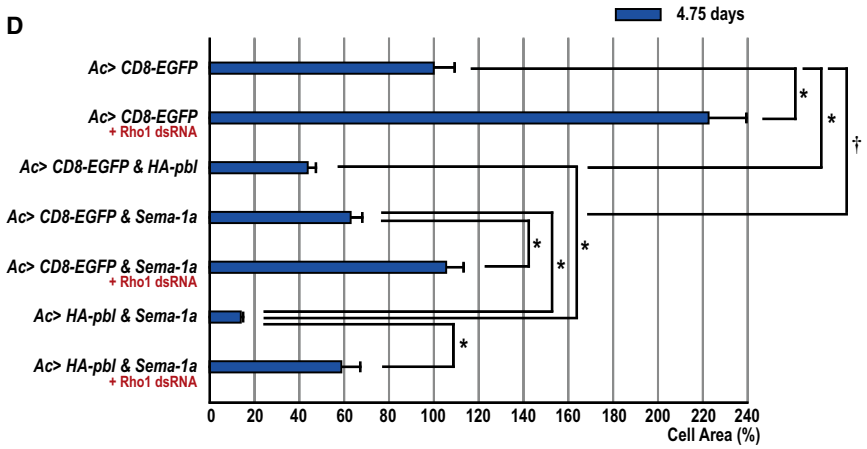

Figure 2. Collaboration between Pebble and Semaphorin-1a in *Drosophila* Cells

(A–C) When cultured on concanavalin A-coated coverslips, most ML-DmBG2 cells become flattened. Overall cellular morphology was visualized with anti-GFP or anti-Sema-1a. ML-DmBG2 cells transfected with membrane-tethered EGFP (*CD8-EGFP*) were stained with rhodamine-phalloidin (red) and anti-GFP (green) (A and A′). ML-DmBG2 cells cotransfected with *HA-pbl* and *Sema-1a* were stained with anti-HA (red) and anti-Sema-1a (green). Ectopically expressed HA-Pbl protein was predominantly localized to the nucleus (B and B′). ML-DmBG2 cells cotransfected with *HA-pbl* and *Sema-1a* were treated with *Rho1* dsRNA for 4.75 days and then stained with anti-HA (red) and anti-Sema-1a (green). Cells with multiple nuclei were frequently observed following *Rho1* dsRNA treatment (C and C′). Scale bar represents 10 μm (A–C).

(D) Quantification of *Sema-1a*, *pbl*, and *Rho1* effects on cell size. CD8-EGFP-expressing cells were used as a control (100% cell area). Error bars represent SEM by t test (*$p < 0.0001$ and †$p = 0.001$).

(E) Proposed interactions between Pbl and p190 with Sema-1a, highlighting potential antagonistic regulation of the small GTPase *Rho1*.

See also Figure S2.

weakly interacts with both PlexA and PlexB (Figures 1A and 1B). However, when we performed these same protein interaction assays using the PlexA ligand Sema-1a, we found that both Pbl and p190 proteins robustly interact with Sema-1a, to a much greater degree than with either PlexA or PlexB (Figures 1A and 1B). These strong interactions are apparently specific since other transmembrane proteins, including *Drosophila* Off-track (Otk), do not coimmunoprecipitate with either Pbl or p190 when coexpressed in S2R+ cells in these same experiments (Figures 1A and 1B). We also observed in coimmunoprecipitation (Co-IP) experiments that neuronally expressed embryonic HA-Pbl and HA-p190 robustly bind to endogenous Sema-1a in vivo (Figure S1A available online). These observations suggest that Pbl and p190 participate in intracellular signaling cascades downstream of Sema-1a (Figure 2E).

Mutations in the Sema-1a Intracellular Domain Reduce Interactions with Pebble and with RhoGAPp190

To further characterize the specificity of these interactions between Sema-1a and Pbl, we mapped the regions of Pbl responsible for interactions with Sema-1a, revealing that the N-terminal domain (NTD), which encompasses two tandem BRCT (BRCA1 C-terminal) domains, is necessary and sufficient for mediating Sema-1a binding (Figure S1B). Through a systematic deletion and mutagenesis analysis of the Sema-1a intracellular domain (ICD), we found that Sema-1a ICD[Δ31–60], in which ICD amino acid residues 31–60 are deleted, and ICD[36G/52A] exhibited differential binding properties to full-length p190 and truncated NTD[Pbl] (Figure 1C; highlighted in red). To address whether this difference is due to the absence of the Pbl C-terminal domain (CTD), we next tested the ability of full-length Pbl and p190 to bind to these mutant forms of the Sema-1a ICD; we observed a significant reduction in Pbl binding to both ICD[Δ31–60] and ICD[36G/52A] (Figure 1D). In addition, the latter mutation also reduced the binding of full-length p190 to the Sema-1a ICD, but to a lesser extent than we observed for Pbl (Figure 1D). These mutations appear to result in reduced access by the Sema-1a ICD to the NTD region of overexpressed full-length Pbl since they lead to increased interaction with the NTD alone (Figure 1C). Therefore, multiple mutations in the Sema-1a ICD are required to affect interactions with both Pbl and p190, defining Sema-1a ICD regions likely to participate in the association of these signaling proteins with Sema-1a.

To address whether Pbl and p190 compete for binding to Sema-1a, we performed competition binding assays in S2R+ cells. Increasing relative levels of Pbl decreased the binding of p190 to Sema-1a by ~50%, whereas increasing relative levels of p190 did not alter Pbl binding to Sema-1a (Figure S1C). These competition data are consistent with our finding that Pbl and p190 both bind to the same Sema-1a domain (Figure 1C), and they suggest that the Pbl association with Sema-1a predominates over p190 association with this same Sema-1a ICD region.

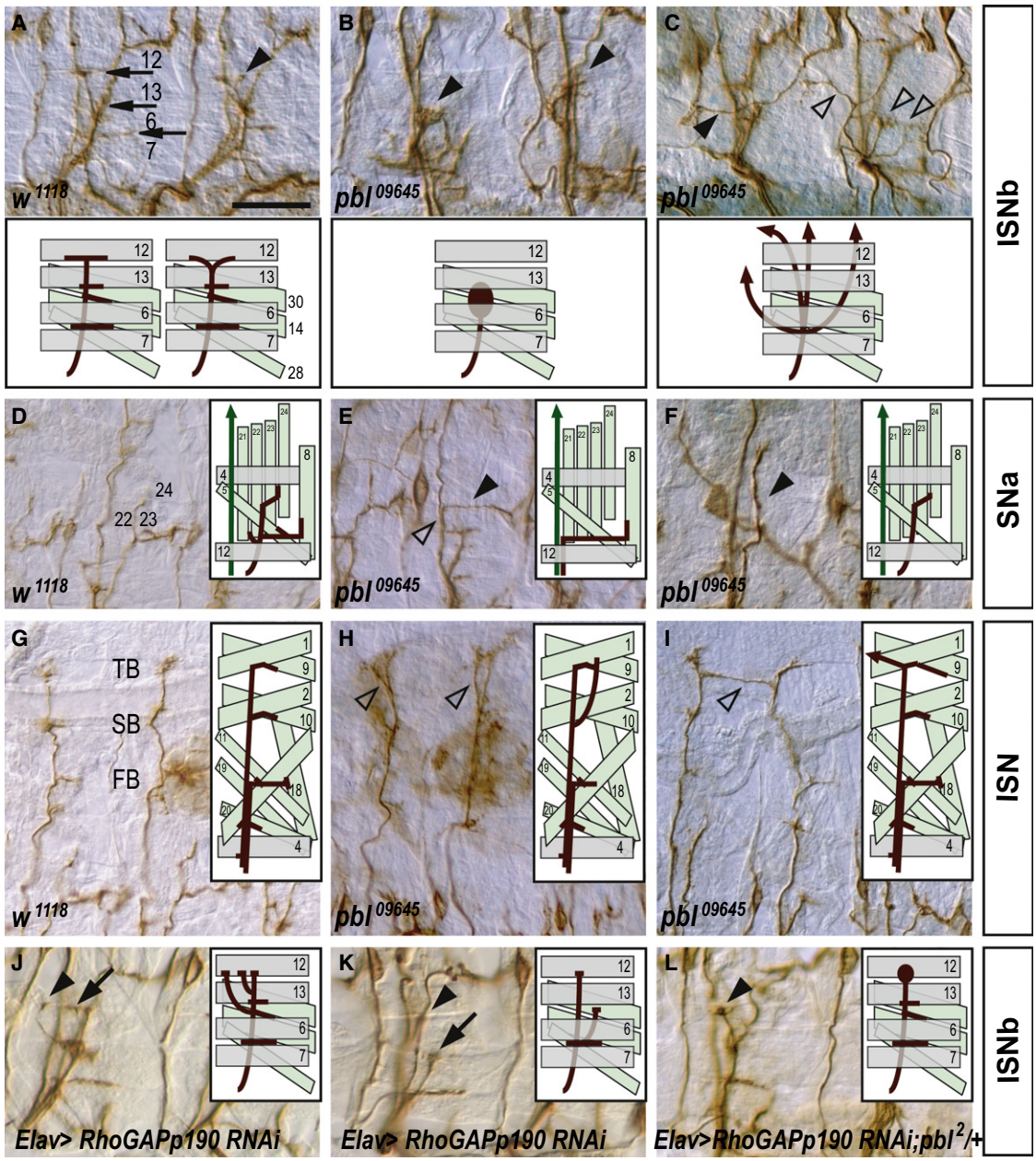

Figure 3. *pebble* and *RhoGAPp190* Are Required for Motor Axon Defasciculation and Target Recognition

Filleted preparations of late stage 16 embryos stained with anti-FasII (the mAb 1D4) to visualize motor axon projection patterns. Anterior is left and dorsal is up. Schematic diagrams showing motor axon guidance in wild-type and indicated mutant backgrounds are presented in each panel.

(A) In wild-type embryos, ISNb axons undergo sequential defasciculation when they arrive between muscles 7 and 6, at the proximal edge of muscle 13, and at muscle 12 to innervate appropriate muscle targets (arrows). Mild premature branching is occasionally observed (arrowhead). Scale bar represents 15 μm.

(B) In *pbl*^{09645} mutants, ISNb axons fail to defasciculate from one another and the ISNb displays an abnormally thick morphology (closed arrowheads). Scale bar represents 15 μm.

(C) ISNb axons in *pbl*^{09645} mutants follow aberrant pathways and fasciculate ectopically with adjacent axons (open arrowheads), including the transverse nerve (TN) (closed arrowhead). Scale bar represents 15 μm.

(D) In wild-type embryos, SNa axons defasciculate and give rise to two branches. The dorsal branch projects to innervate muscles 22–24 with two characteristic turns, while the lateral branch extends posteriorly and innervates its target muscles. Scale bar represents 20 μm.

(E) In *pbl*^{09645} mutants, SNa axons follow the ISN trajectory (detour phenotype, open arrowhead) and the dorsal branch of the SNa is often missing (closed arrowhead). Scale bar represents 20 μm.

(F) In *pbl*^{09645} mutants, lateral SNa branches are missing (closed arrowhead). Scale bar represents 20 μm.

(G) In wild-type embryos, ISN axons project to the dorsal-most muscle fields and elaborate three distinct branches: first (FB), second (SB), and third (TB). Scale bar represents 20 μm.

Pebble and Sema-1a Collaborate to Regulate Cell Size through Rho1 in *Drosophila* Cells In Vitro

In *Drosophila* S2 cells, RNAi-mediated depletion of *Rho1* induces a dramatic increase in cell size (Rogers and Rogers, 2008). Recent analysis of photoreceptor axon guidance in *Drosophila* shows that *Rho1* is involved in Sema-1a reverse signaling (Yu et al., 2010). Therefore, we utilized a *Drosophila* cell line with neuronal characteristics, called ML-DmBG2-c2 (Ui et al., 1994), to examine links between Sema-1a signaling and *Rho1*. We depleted endogenous Rho1 in these cells using double-stranded RNA (dsRNA) for 4.75 days and observed a ~2-fold increase in cell size (Figure 2D). In contrast, overexpression of Pbl, which positively regulates Rho1, caused a ~2-fold reduction in cell size. Interestingly, ectopic expression of Sema-1a in these cells also led to a significant reduction in cell size, suggesting a link between Sema-1a signaling and Rho1 activity through the action of Pbl. This idea is supported by the observation that Sema-1a-induced reduction in cell size was suppressed by depleting Rho1 (Figure 2D). To further explore Sema-1a-mediated modulation of Rho1 activity through Pbl, we coexpressed Sema-1a and Pbl and observed a dramatic reduction in cell size (Figures 2B and 2D); these Pbl gain-of-function (GOF)-mediated reductions in cell size were not the result of affecting cytokinesis, a known *pbl* function (Prokopenko et al., 1999) (data not shown). This synergistic Sema-1a-Pbl reduction in cell size was also significantly attenuated by *Rho1* depletion (Figures 2C and 2D). These results suggest that Sema-1a and Pbl collaborate to trigger cell size reduction through the activation of Rho1 in *Drosophila* neuronal cells in vitro (Figure 2E).

We also asked whether or not an antagonistic relationship exists between Sema-1a and p190 in these cells. As expected, overexpression of p190 resulted in an increase in cell size, and the average size of cells coexpressing both p190 and Sema-1a is significantly reduced as compared to cells expressing p190 alone (Figure S2). Therefore, Sema-1a overexpression is epistatic to p190 overexpression with respect to cell size in vitro.

pebble Regulates Motor Axon Defasciculation and Target Recognition

To determine whether *pbl* plays a role in axon pathfinding, we examined motor axons in hypomorphic *pbl* alleles, referred to here as pbl^{09645} and $pbl^{KG07669}$, that have P element insertions in the 5′-untranslated region of *pbl* (Figure S3A) (Bellen et al., 2004; Prokopenko et al., 2000). Embryos homozygous for these hypomorphic *pbl* alleles show highly penetrant peripheral nervous system (PNS) axon guidance defects (Figures 3A–3I and 4A). In wild-type embryos, ISNb axons first defasciculate from the ISN near the lateral margins of the CNS and extend to the ventrolateral muscle field (Keshishian et al., 1996). Subsequently, ISNb axons defasciculate from one another and establish presynaptic arborizations between muscles 7 and 6, and at the proximal edges of muscles 13 and 12 (arrows in Figure 3A). ISNb axons in pbl^{09645} homozygous mutant embryos show highly penetrant guidance defects (98% of mutant hemisegments; Figure 4A). In pbl^{09645} homozygous mutants, ISNb axons often fail to defasciculate from one another, resulting in a hyperfasciculated phenotype and a failure to reach their muscle targets (Figure 3B). In addition, we frequently observed in *pbl* mutant embryos that ISNb axons fail to either navigate along their normal trajectories or innervate their normal target muscles, even though these motor axon growth cones do reach the vicinity of their target regions (an apparent target recognition error; Figures 3B and 3C). These fasciculation and target recognition errors are not seen in wild-type embryos (Figure 3A).

Most axons in the segmental nerve a (SNa) pathway also exhibited severe defasciculation defects and/or target recognition failure in pbl^{09645} homozygous mutant embryos (90% of hemisegments; Figures 3E, 3F and 4A). In wild-type embryos, SNa axons separate from the SN nerve and project to the dorsolateral muscle field (Landgraf et al., 1997; Van Vactor et al., 1993). Subsequent defasciculation of SNa axons gives rise to a dorsal and lateral branch. The dorsal branch establishes synaptic arborizations between muscles 21, 22, 23, and 24, while the lateral branch innervates muscle 5 and 8 (Figure 3D). In pbl^{09645} mutants, the dorsal or lateral SNa branches were often missing (Figures 3E and 3F). These SNa phenotypes are not observed in wild-type embryos (Figure 3D).

Wild-type ISN axons navigate to the dorsal-most muscle field and form three distinctive branches: the first (FB), second (SB), and third branch (TB) (Figure 3G). The ISN axons in pbl^{09645} homozygous mutant embryos exhibit a failure of correct muscle target recognition. The first or second branches of the mutant ISN motor axons often extend dorsally beyond the correct muscle fields (Figure 3H). Occasionally, mutant ISN axons cross the segment boundary and fasciculate with adjacent ISN axons (Figure 3I). To confirm that these defects in motor axon guidance result from the loss of *pbl* function, we characterized homozygous mutant embryos from a second P element insertion line called $pbl^{KG07669}$ (Figure S3A). These embryos also displayed highly penetrant axon guidance defects in the PNS, although they were somewhat less severe than those observed in pbl^{09645} mutants (Figure 4A). Furthermore, we found that embryos transheterozygous for pbl^{09645} and $pbl^{KG07669}$ showed similar penetrance of these defects but less severity compared to pbl^{09645} mutants (data not shown). These genetic data show that *pbl* plays an important role in establishing normal neuromuscular connectivity during embryogenesis.

(H) In pbl^{09645} mutants, ISN axons defasciculate prematurely (open arrowheads). Scale bar represents 20 μm.
(I) In pbl^{09645} mutants, ISN axons often cross the segment boundary and ectopically contact the adjacent ISN (open arrowhead). Scale bar represents 20 μm.
(J) RNAi-mediated knockdown of *p190* causes premature defasciculation (arrow) and probably a defect in muscle target recognition (arrowhead) since two ISNb axons are thought to target the proximal edge of muscle 12. Scale bar represents 15 μm.
(K) Premature defasciculation rarely initiates before ISNb axons reach muscle 6 (arrow); an innervation defect is also shown (arrowhead). Scale bar represents 15 μm.
(L) RNAi-mediated knockdown of *p190* in a heterozygous pbl^{2} background leads to a characteristic defasciculation defect at the edge of muscle 12 (arrowhead). Scale bar represents 15 μm.

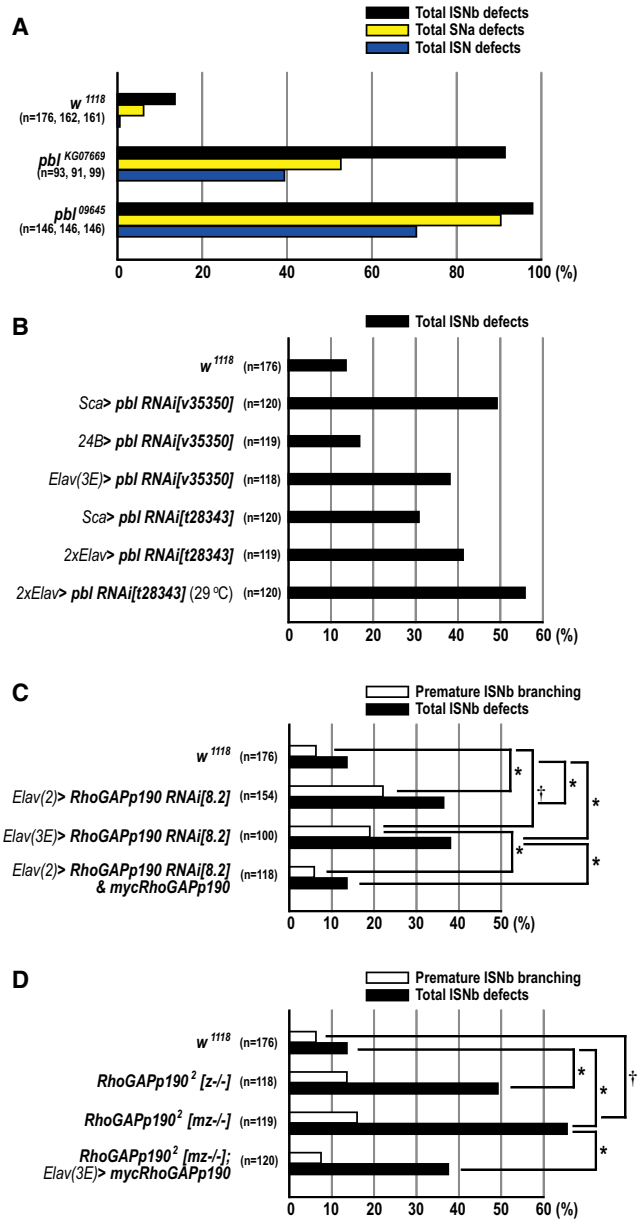

Figure 4. Neuronal *pebble* and *RhoGAPp190* Are Required for Motor Axon Guidance

(A) The percentages of ISNb, SNa, and ISN guidance defects in w^{1118} (wild-type), $pbl^{KG07669}$, and pbl^{09645} embryos.

(B) Total ISNb defects in embryos in which endogenous *pbl* is knocked down in either neuroblasts, postmitotic neurons, or all muscle cells using *Sca-GAL4*, *Elav-GAL4*, or *24B-GAL4* respectively.

(C) The percentages of total ISNb defects (closed bars) and premature ISNb branching phenotypes (open bars) of the ISNb in w^{1118}, *p190* knockdown, and rescue embryos (*$p < 0.001$ and †$p < 0.01$, χ^2 test).

(D) The percentages of total ISNb defects (closed bars) and premature ISNb branching phenotypes (open bars) in w^{1118}, $p190^2$, and rescue embryos. z−/− and mz−/− indicate zygotic null, and maternal/zygotic null for *p190*, respectively (*$p < 0.001$ and †$p = 0.012$, χ^2 test). n = the number of abdominal hemisegments scored for each genotype (A–D).

See also Figures S4 and S5.

In addition to motor axon pathfinding defects in the PNS, pbl^{09645} homozygous mutants showed 2.6% total CNS defects, $pbl^{KG07669}$ homozygous mutants displayed 0.0% total CNS defects, and mutants transheterozygous for pbl^{09645} and $pbl^{KG07669}$ showed 0.93% total CNS defects (data not shown). These findings indicate that *pbl* contributes very little to CNS axon guidance.

Neuronal *pebble* Is Required for Motor Axon Pathfinding

To assess whether or not the defects we observe in motor axon pathfinding result from the loss of *pbl* function in muscles or in neurons, we expressed a *HA-pbl* transgene in all muscles of pbl^{09645} mutant embryos using the *24B-GAL4* driver (Luo et al., 1994). These embryos showed motor axon pathfinding defects similar to those seen in pbl^{09645} mutants (Figures S3F and S3G). In contrast, expression of *HA-pbl* in neurons using *Sca-GAL4*, which is expressed in all neuroblasts and their progeny (Klaes et al., 1994), led to partial but significant rescue of *pbl* loss-of-function (LOF) phenotypes in both ISNb and SNa, but not ISN, motor neuron pathways (Figures S3E and S3G). For example, in pbl^{09645} mutant embryos, ISNb axons frequently failed to innervate muscles 6/7 (81.5% of hemisegments; Figure S3G), whereas neuronal expression of *HA-pbl* in pbl^{09645} mutant embryos strongly suppressed these innervation defects (34.1% of hemisegments; Figures S3E and S3G). We find that the $pbl^{KG07669}$ allele, which exhibits highly penetrant axon pathfinding defects in the PNS (Figure 4A), does not alter cell fate specification or proliferation of CNS neurons compared to wild-type embryos (Figures S4G and S4H, and data not shown). Furthermore, in $pbl^{KG07669}$ homozygous mutants, the embryonic pattern and morphology of muscles 21–24 and ventrolateral muscles is apparently normal with respect to muscle fiber size, shape, and position (Figures S4B and S4E). These data suggest that neuronal, but not muscle, functions of *pbl* contribute to correct ISNb and SNa motor axon guidance.

To further address whether or not neuronal Pbl is required for motor axon pathfinding, we used a transgenic RNA interference (RNAi) approach. When the *pbl* gene was knocked down by overexpression of *pbl RNAi[v35350]* or *pbl RNAi[t28343]* (Supplemental Experimental Procedures; Figure S5) transgenes using *Sca-GAL4*, projection patterns of ISNb axons showed increased fasciculation and defects in target recognition (49.2% or 30.8% of hemisegments, respectively; Figure 4B). Knockdown of *pbl* in all muscles using *24B-GAL4* resulted in no significant ISNb pathfinding defects (Figure 4B). To address whether *pbl* axon guidance and cytokinesis functions are separable, we knocked down *pbl* gene function using the postmitotic driver *Elav-GAL4*. Embryos overexpressing *pbl RNAi[v35350]* under the control of *Elav-GAL4* exhibited ISNb defects in 38% of hemisegments (Figure 4B). A similar phenotype was observed with the *t28343 RNAi* line under the control of two copies of *Elav-GAL4*. Since the GAL4/UAS system is temperature-sensitive, we allowed these embryos to develop at 29°C to increase GAL4-mediated expression of *pbl* RNAi and observed an increase in the penetrance of motor axon pathfinding defects as compared to 25°C (55.8% versus 41.2%; Figures 4B, S3C, and S3D). These data strongly suggest that neuronal Pbl is required postmitotically for normal motor axon pathfinding.

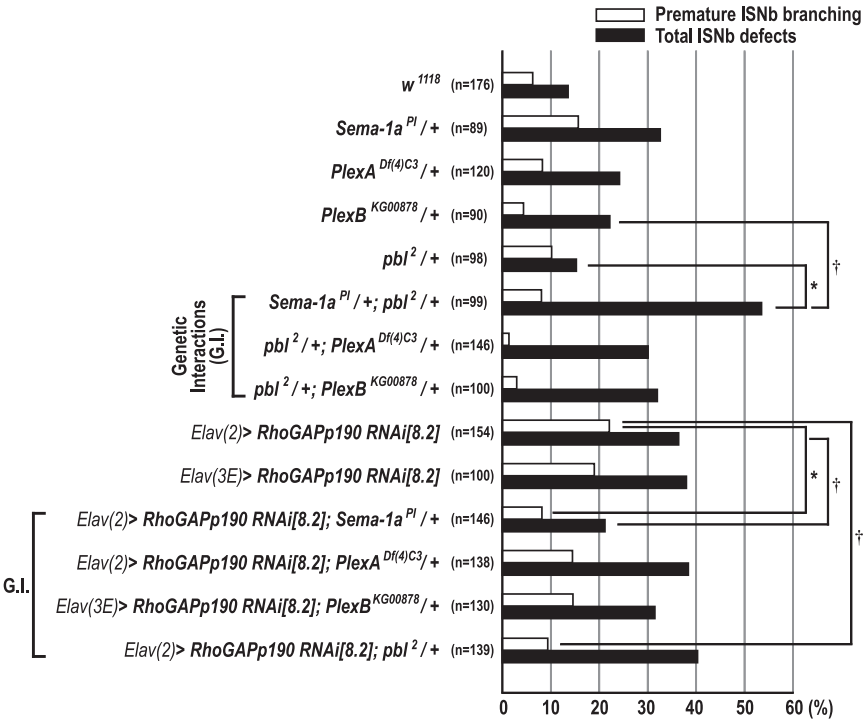

Figure 5. Genetic Interactions among *Sema-1a*, *pebble*, and *RhoGAPp190* Mutants

Premature ISNb branching phenotypes (open bars) and total ISNb defects (closed bars) in embryos with indicated genotypes (*$p < 0.001$ and †$p < 0.01$, χ^2 test). Total ISNb defects in embryos transheterozygous for *Sema-1a* and *pbl* are greater than those observed in either *Sema-1a* or *pbl* heterozygous embryos. Removing one copy of *Sema-1a* significantly suppresses *p190* knockdown-mediated premature ISNb branching phenotypes and also total ISNb defects. Removing one copy of *pbl* also leads to significant suppression of *p190* knockdown-mediated premature ISNb branching phenotypes. n = the number of abdominal hemisegments scored for each genotype.

See also Figure S6.

Neuronal *RhoGAPp190* Is Also Required for Motor Axon Pathfinding

Since we observed that p190, like Pbl, also exhibits a strong physical association with Sema-1a and that two potential *p190* enhancer GAL4 lines drive reporter expression in the CNS (Figures S3H–S3J), we examined the role played by p190 in motor axon pathfinding using transgenic RNAi lines (Billuart et al., 2001). Overexpression of the *p190* RNAi transgene using *Elav-GAL4* resulted in premature defasciculation of ISNb axons prior to reaching muscle 13, and sometimes muscle 6: reflecting either increased defasciculation or a defect in muscle target recognition (~20% of hemisegments; Figures 3J, 3K, 4C, and S6). This premature branching phenotype was rescued to wild-type levels when one copy of a *UAS-mycp190* transgene (Billuart et al., 2001) was introduced along with *p190* RNAi (5.9% of hemisegments; Figure 4C). Furthermore, when premature branching is observed in wild-type embryos it is qualitatively distinct from what we observe following *p190* LOF, often occurring between the ventral and dorsal surfaces of muscle 13 rather than prior to ISNb arrival at muscle 13 (compare arrowhead in Figure 3A to arrows in Figures 3J and 3K). In addition, premature ISNb branching phenotypes qualitatively and quantitatively similar to those we observe in *p190* RNAi lines were noted in $p190^2$ maternally and zygotically-derived null alleles, and total ISNb defects were significantly rescued by reintroduction of the neuronal *mycp190* transgene (Figure 4D). These results show that neuronal *p190* is required postmitotically for motor axon pathfinding.

Semaphorin-1a-Mediated Axon Guidance Is Regulated Positively by *pebble* and Negatively by *RhoGAPp190*

To test whether *pbl* plays a role in Sema-1a-mediated motor axon guidance, we investigated genetic interactions between *pbl* and *Sema-1a*, *PlexA*, and *PlexB*. When either a *PlexA* or *PlexB* null allele was introduced into pbl^2 heterozygotes, total ISNb and premature branching defects were not significantly affected. However, when a single *Sema-1a* mutant allele was introduced into the *pbl* heterozygous background, we observed a significant increase in the frequency of total ISNb defects (53.5%) compared to embryos heterozygous for either *Sema-1a* or *pbl*, although premature branching was apparently unaffected (Figure 5). Similar patterns of genetic interactions were also observed with pbl^3, and pbl^5 null alleles (Figure S6). The amino acid Val531, which is changed to aspartate in the pbl^5 mutant (V531D), is located within the Pbl DH domain and is known to be required for nucleotide exchange activity in the DH domains of other GEFs (Liu et al., 1998; Prokopenko et al., 1999). These results suggest that Sema-1a and Pbl act together in the same signaling pathway to promote motor axon guidance through the regulation of Pbl GEF activity and, since similar genetic interactions are not observed with *PlexA*, that Pbl functions as an intracellular mediator downstream of Sema-1a rather than PlexA. However, heterozygosity for $pbl^{KG07669}$ significantly enhances the *Sema-1a* null phenotype (Figure S6), indicating that additional Pbl guidance functions cooperate with Sema-1a signaling.

Since p190 physically associates with Sema-1a, we next asked whether or not p190 is involved in Sema-1a-mediated motor axon guidance. First, we observed that the *p190* RNAi phenotype was suppressed by loss of a single copy of *Sema-1a*: from 22.1% to 8.2% for premature ISNb branching, and from 36.4% to 21.2% for total ISNb defects (Figure 5). In contrast, *PlexA* or *PlexB* null alleles did not affect the *p190* RNAi phenotype. These suppressive genetic interactions between *p190* and *Sema-1a* were also observed using a different *p190* RNAi line and the $p190^2$ null allele (Figure S6). Therefore, *p190* functions to antagonize Sema-1a signaling, but not *PlexA* or *PlexB* signaling. This is consistent with physical association between p190 and Sema-1a being stronger than with either

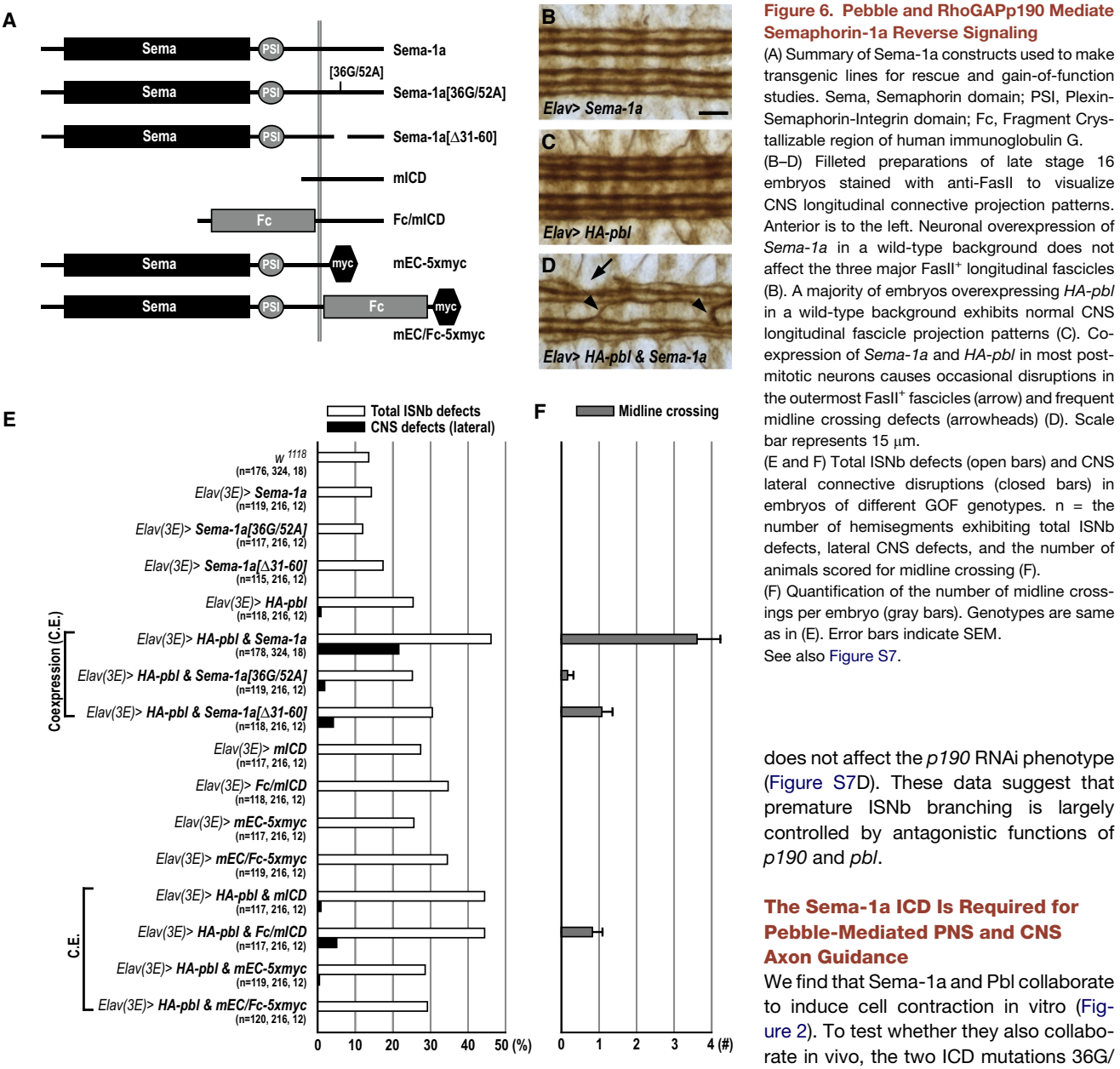

Figure 6. Pebble and RhoGAPp190 Mediate Semaphorin-1a Reverse Signaling

(A) Summary of Sema-1a constructs used to make transgenic lines for rescue and gain-of-function studies. Sema, Semaphorin domain; PSI, Plexin-Semaphorin-Integrin domain; Fc, Fragment Crystallizable region of human immunoglobulin G.

(B–D) Filleted preparations of late stage 16 embryos stained with anti-FasII to visualize CNS longitudinal connective projection patterns. Anterior is to the left. Neuronal overexpression of *Sema-1a* in a wild-type background does not affect the three major FasII^{+} longitudinal fascicles (B). A majority of embryos overexpressing *HA-pbl* in a wild-type background exhibits normal CNS longitudinal fascicle projection patterns (C). Co-expression of *Sema-1a* and *HA-pbl* in most postmitotic neurons causes occasional disruptions in the outermost FasII^{+} fascicles (arrow) and frequent midline crossing defects (arrowheads) (D). Scale bar represents 15 μm.

(E and F) Total ISNb defects (open bars) and CNS lateral connective disruptions (closed bars) in embryos of different GOF genotypes. n = the number of hemisegments exhibiting total ISNb defects, lateral CNS defects, and the number of animals scored for midline crossing (F).

(F) Quantification of the number of midline crossings per embryo (gray bars). Genotypes are same as in (E). Error bars indicate SEM.

See also Figure S7.

PlexA or PlexB (Figure 1B). Taken together, these genetic interaction data suggest that Pbl and p190 exert opposing control over Sema-1a-mediated motor axon.

Next, we examined whether *pbl* and *p190* genetically interact. When a single *pbl*^{2} mutant allele was introduced to *p190* RNAi knockdown embryos, the premature branching phenotype was significantly reduced, from 22.1% to 9.4% (Figure 5). In these embryos, we also observed a significant increase in motor axon defasciculation defects (excluding premature branching phenotypes) at the last ISNb choice point (Figures 3L and 5). To test whether increasing Pbl levels affects premature ISNb branching phenotypes, we overexpressed *HA-pbl* alone or with coexpression of *p190* RNAi in neurons. Increasing Pbl leads to a significant increase in premature branching phenotypes, but does not affect the *p190* RNAi phenotype (Figure S7D). These data suggest that premature ISNb branching is largely controlled by antagonistic functions of *p190* and *pbl*.

The Sema-1a ICD Is Required for Pebble-Mediated PNS and CNS Axon Guidance

We find that Sema-1a and Pbl collaborate to induce cell contraction in vitro (Figure 2). To test whether they also collaborate in vivo, the two ICD mutations 36G/52A and Δ31–60, which show a 33% and 44% reduction in binding to Pbl, respectively (Figure 1D), were introduced into the wild-type Sema-1a protein. We then overexpressed *HA-pbl* and modified *Sema-1a* transgenes using the postmitotic driver *Elav-GAL4*. When both *Sema-1a* and *pbl* transgenes were coexpressed in neurons, ISNb defects increased from 25.4% to 46.1%; interestingly, CNS defects in the lateral-most FasII^{+} longitudinal connective increased ~20-fold, from 0.9% to 21.6%, when compared to overexpression of *HA-pbl* alone (Figures 6B–6E). In embryos expressing both Sema-1a and Pbl in postmitotic neurons, we also observed a dramatic increase in ectopic CNS midline crossing: from 0.0 to 3.6 crossings per embryo (Figures 6D and 6F). These synergistic effects were not observed in embryos coexpressing HA-Pbl and PlexA, suggesting they result from specific signaling

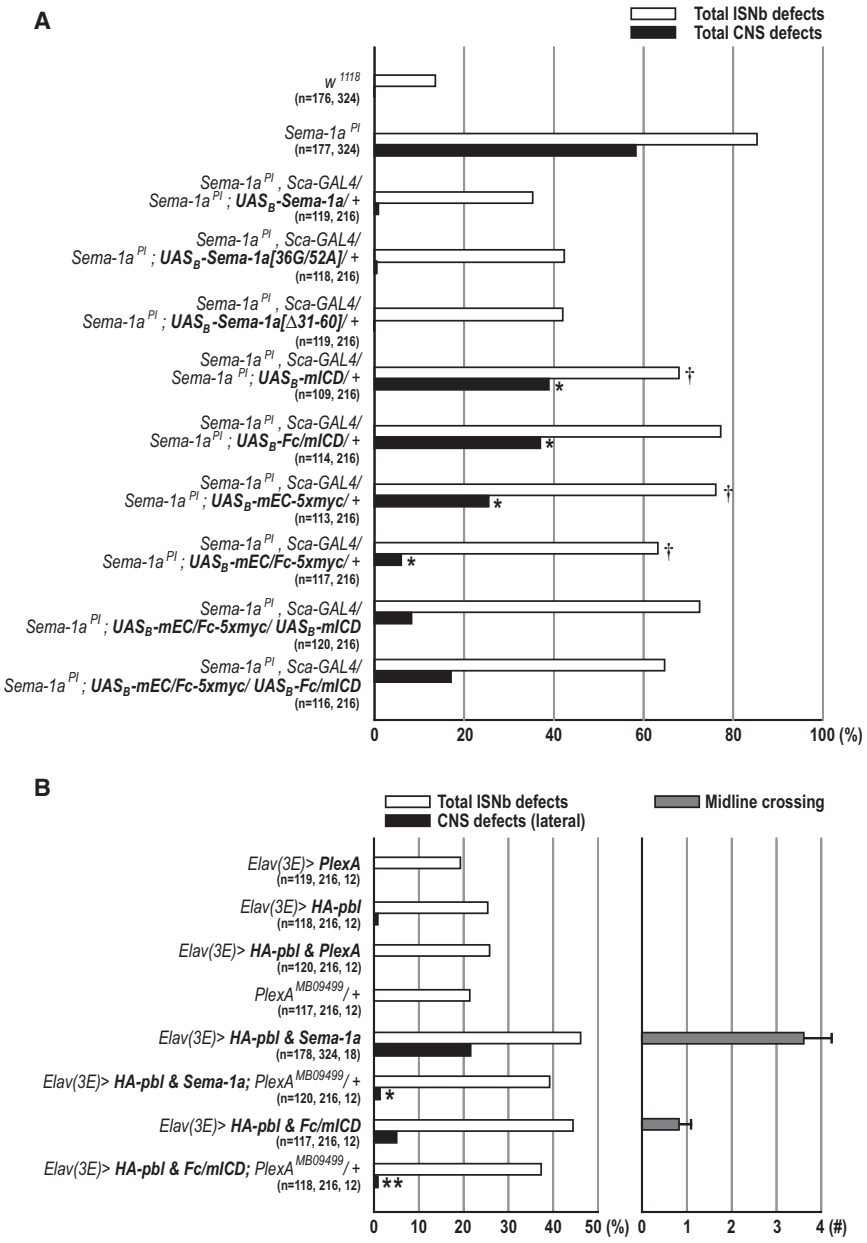

Figure 7. Both Forward and Reverse Sema-1a Signaling Is Required for Correct Motor Axon Guidance in the PNS

(A) Rescue of *Sema-1a* axon guidance phenotypes with various modified Sema-1a proteins. Embryos with indicated genotypes were scored for the frequency of total ISNb defects (open bars) and total CNS defects (closed bars) (*$p < 0.0001$ and †$p = 0.05$, χ^2 test). n = the number of hemisegments scored for total ISNb defects and CNS defects.

(B) Genetic interactions among *PlexA*, *Sema-1a*, and *pbl*. Total ISNb branching phenotypes (open bars), lateral longitudinal CNS defects (closed bars), and midline crossing phenotypes (gray bars) were scored in embryos of the indicated genotypes (*$p = 0.0001$ and **$p = 0.0245$; χ^2 test). n = the number of hemisegments scored for total ISNb defects, lateral CNS defects, and the number of animals scored for midline crossing. Error bars indicate SEM.

See also Figure S8.

interactions between Pbl and Sema-1a (Figure 7B). A truncated form of Sema-1a (mEC-5xmyc, Figure 6A), which lacks the entire ICD, did not exhibit any synergistic interactions with HA-Pbl (Figure 6E), commensurate with our observations that the ICD binds to Pbl (Figure 1D). Next, we examined two *Sema-1a* mutant transgenes harboring the mutations 36G/52A and Δ31–60. When these altered Sema-1a proteins were coexpressed with *HA-pbl*, total ISNb and CNS defects were not significantly increased above *HA-pbl* overexpression alone (Figures 6E and 6F). Coexpression of *Sema-1a[Δ31–60]* with *HA-pbl* did cause a modest increase in lateral CNS defects (4.2%) and midline crossing phenotypes (1.1 per animal); these defects are far less robust than those observed with coexpression of wild-type Sema-1a and Pbl, and they are consistent with our observation that the Pbl NTD is able to bind in vitro to ICD[Δ31–60] (Figures 6E, 6F, and 1C). In addition, the synergistic Sema-1a-Pbl-mediated increase in premature ISNb branching phenotypes in vivo, and also the reduction in cell size in vitro, was significantly attenuated when either ICD Sema-1a mutant was coexpressed with HA-Pbl (Figures S7D and S2). These data show that *pbl* and *Sema-1a* can collaborate in these GOF paradigms to affect axon guidance in vivo and cell size in vitro, and that this likely occurs through interactions between Pbl and the Sema-1a ICD.

Semaphorin-1a Bidirectional Signaling Is Required for Embryonic Motor Axon Pathfinding

The *Sema-1a^{PI}* LOF allele (Yu et al., 1998) has the capacity to impair both forward and reverse signaling. However, it is not clear whether Sema-1a bidirectional signaling is required for PNS and/or CNS axon guidance in embryonic development. Therefore, we made a series of constructs that express truncated and chimeric Sema-1a proteins and then assessed these Sema-1a transgenes for their ability to rescue PNS and CNS guidance defects in homozygous *Sema-1a* mutants (Figure 6A). *Sema-1a* homozygous mutants show dramatically increased guidance defects in the ISNb and most lateral FasII$^+$ CNS longitudinal axon pathways (Figures 7A, S3B, and S8C). Interestingly, neuronal expression of the mEC/Fc-5xmyc chimeric receptor, which lacks the entire ICD and thus reverse signaling activity, caused a dramatic reduction in CNS defects compared to the *Sema-1a* null phenotype (6.0% versus 58.5%), while the mEC-5xmyc truncated

protein led to an intermediate reduction (25.5%; Figure 7A). However, significant but modest rescue of CNS defects was observed in embryos carrying either mICD or Fc/mICD mutant Sema-1a proteins, which lack forward signaling activity (Figure 7A). These results demonstrate that multimerization of the Sema-1a extracellular domain is largely sufficient to mediate *Sema-1a* functions in CNS axon guidance. Furthermore, we found that neuronal expression of either of these signaling mutant transgenes partially rescued *Sema-1a* null ISNb pathway phenotypes (Figure 7A). In particular, neuronal expression of mEC/Fc-5xmyc, which should allow forward but not reverse signaling, resulted in only modest rescue of ISNb defects but significant rescue of CNS defects, suggesting an essential role for Sema-1a-mediated reverse signaling in peripheral axon guidance. Next, we performed additional rescue experiments in order to examine whether the introduction of both forward (mEC/Fc-5xmyc) and reverse (mICD or Fc/mICD) signaling mutant transgenes together can further rescue Sema-1a ISNb phenotypes. However, simultaneous expression of these transgenes did not lead to additional rescue of *Sema-1a* null PNS phenotypes, as compared to neuronal expression of either single transgene (Figure 7A). Given that Sema-1a functions as a ligand for PlexA in the PNS (forward signaling; Winberg et al., 1998), these complementation analyses strongly suggest that both the extracellular and intracellular Sema-1a domains, and therefore the coordinated action of bidirectional signaling, are necessary for Sema-1a-mediated motor axon guidance.

Pebble Mediates Semaphorin-1a Reverse Signaling

Since overexpression of wild-type Sema-1a synergistically enhances *pbl* misexpression phenotypes in both the PNS and CNS (Figures 6B–6F), we reasoned that if this synergistic enhancement occurs through the potentiation of reverse signaling, the Sema-1a intracellular domain alone should recapitulate the synergistic enhancement we see when wild-type Sema-1a is coexpressed with *HA-pbl*. We found in our GOF analysis that expression of mICD or Fc/mICD did indeed increase *pbl* GOF ISNb phenotypes to a similar level as wild-type Sema-1a, but produced only mild defects in CNS patterning (Figures 6E and 6F). However, overexpression of the Sema-1a extracellular domain (mEC-5xmyc or mEC/Fc-5xmyc) did not affect *pbl* GOF phenotypes in either ISNb or CNS axon guidance. These in vivo GOF data strongly suggest that Pbl mediates Sema-1a reverse signaling.

To address further Sema-1a receptor function and its regulation by Pbl, we performed additional GOF experiments utilizing *apterous-GAL4* (*apGAL4*), which drives expression of GAL4 in only three neurons per hemisegment; these neurons extend axons longitudinally and do not cross the CNS midline (O'Keefe et al., 1998), and Sema-1a signaling mutants (Figure S7A). Coexpression of Sema-1a and HA-Pbl in the apterous neurons frequently leads to a failure of fasciculation among these apterous^{+} axons and results in a "midline crossing" phenotype (Figure S7B). Similar fasciculation defects in the apterous^{+} neurons are also found in embryos coexpressing Fc/mICD and HA-Pbl (Figure S7C). However, the axon fasciculation defects observed in embryos coexpressing mEC/Fc-5xmyc (Sema-1a ecto-domain) and HA-Pbl are not significantly different from those observed in *apGAL4*/+ animals (Figure S7C). These results provide additional support for Sema-1a functioning as a receptor that signals via Pbl.

To complement these genetic interaction data, we performed similar GOF studies in *Drosophila* cells in vitro. Consistent with our in vivo observations, we found that Pbl collaborates with Fc/mICD, but not with mEC/Fc-5xmyc, to induce cell size reduction (Figure S2). Taken together with our protein-protein interaction and genetic complementation data (Figures 1 and 7A), these GOF studies strongly suggest that Pbl mediates Sema-1a reverse signaling through direct interaction with the intracellular domain of Sema-1a.

To determine whether PlexA functions as a ligand for Sema-1a-mediated reverse signaling, one copy of a *PlexA* loss-of-function mutation (*PlexA*^{MB09499}; Figure S8) (Bellen et al., 2011) was introduced into embryos coexpressing *Sema-1a* and *HA-pbl*. Interestingly, the CNS defects observed following coexpression of both *Sema-1a* and *HA-pbl* transgenes were strongly suppressed in a *PlexA* heterozygous background (Figure 7B). Similarly, removing one copy of *PlexA* led to a significant suppression of *Fc/mICD* and *HA-pbl* gain-of-function CNS defects, indicating that this PlexA-mediated suppression is not dependent upon the Sema-1a extracellular domain (Figure 7B). However, we did not observe a significant suppression of ISNb defects in embryos that coexpress either *Sema-1a* or *Fc/mICD* along with *HA-pbl* in a *PlexA* heterozygous background, consistent with previous observations that *PlexA* functions as a Sema-1a receptor to mediate repulsive signaling during neuromuscular development (Figure 7B; Winberg et al., 1998). These results suggest that PlexA functions in parallel with Sema-1a reverse signaling in the CNS, and further, that PlexA does not function as a major ligand for Sema-1a in both the PNS and the CNS (Figure 8).

DISCUSSION

We describe here a signaling pathway whereby the transmembrane guidance cue Sema-1a regulates axon-axon interactions, providing insight into links between guidance cue recognition and subsequent intracellular signaling events. We find that the RhoGTPase regulators Pbl and p190 physically associate with the cytoplasmic domain of Sema-1a, and our genetic analyses support a role for these signaling molecules in mediating Sema-1a reverse signaling during embryonic axon pathfinding in *Drosophila*.

Function and Regulation of *pebble* and *RhoGAPp190* in Motor Axon Pathfinding

We find that the *pbl*^{09645} hypomorphic allele shows highly penetrant defects in target recognition by ISNb axons (88.4% of hemisegments) in addition to an increased fasciculation phenotype (54.1% of hemisegments). The function of Pbl in target recognition might be directly associated with Sema-1a-mediated defasciculation, since 41.1% of the hemisegments in *pbl*^{09645} homozygous mutants exhibit both target recognition errors and severely increased fasciculation. In general, repulsive signaling can be selectively activated to mediate axon-axon defasciculation at choice points, whereas attractive target

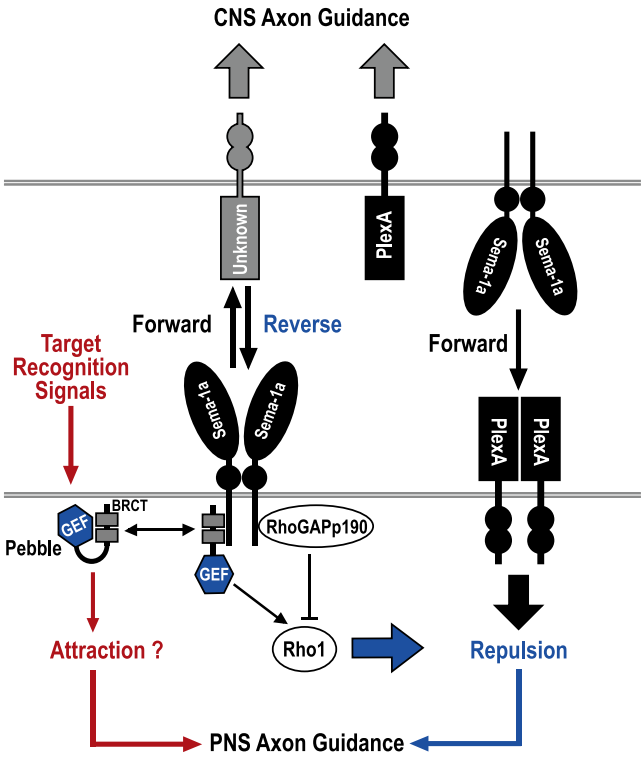

Figure 8. The Control of Semaphorin-1a Reverse Signaling by Pebble and RhoGAPp190

Repulsive guidance signals specified by Sema-1a bidirectional signaling play an important role in sculpting *Drosophila* neuromuscular connectivity. In our model, Sema-1a forward signaling largely contributes to CNS axon guidance, whereas both forward and reverse signaling are required to induce axon-axon repulsion at specific pathway choice points in the PNS. In the PNS, two direct but opposing regulators of Rho family small GTPases, *pbl* and *p190*, are required for attractive target recognition processes that guide motor axons before reaching, or after leaving, guidance choice points. Furthermore, these proteins mediate Sema-1a reverse signaling through the control of Rho1 activity at guidance choice points and likely participate in the recognition of these choice points by axonal growth cones, an essential prerequisite for selective axon-axon defasciculation mediated by repulsive signaling pathways. We propose that Pbl links choice-point recognition signaling and Sema-1a reverse signaling, and further, that Sema-1a reverse signaling collaborates in parallel with receptor functions of PlexA to induce selective axon-axon repulsion. In addition, Pbl not only competes, but also collaborates, with p190 to regulate Sema-1a reverse signaling in a context-dependent manner. Sema-1a/PlexA-mediated repulsive signaling and target recognition signaling are likely integrated and coordinated by *pbl* and *p190*, both spatially and temporally, so as to establish precise connections between motoneurons and their muscle targets.

recognition cues most likely guide axons before reaching, or after leaving, guidance choice points (Kolodkin and Tessier-Lavigne, 2011). Furthermore, the recognition of choice points by axonal growth cones is an essential prerequisite for selective axon-axon defasciculation mediated by repulsive signaling pathways.

Here, we propose that Pbl links choice-point recognition signaling and Sema-1a/PlexA repulsive signaling (Figure 8). In this scenario, Pbl is primed by choice-point recognition signals, and primed Pbl is subsequently activated through direct interaction with the Sema-1a signaling complex. The priming event might be related to the accessibility of the Sema-1a ICD to the BRCT domains of Pbl. In support of this idea, we observed that two mutant forms of Sema-1a (Sema-1a[36G/52A] and Sema-1a[Δ31–60]) that exhibit strong reductions in binding to full-length Pbl and also reductions in synergistic genetic interactions with HA-Pbl in GOF studies can fully rescue the Sema-1a mutant phenotype in complementation tests (Figure 7A). However, these mutations introduced into Sema-1a ICD do not affect the ability of this modified Sema-1a ICD to bind to truncated Pbl NTD proteins that lack the C-terminal domain which, based on the work of others (Kim et al., 2005; Saito et al., 2004), is known to mediate auto-inhibitory intramolecular interactions with BRCT domains. Therefore, endogenous Pbl may undergo a conformational change to relieve auto-inhibitory interactions and/or increase membrane targeting as a result of choice-point recognition, and this could increase the accessibility and binding of the Pbl BRCT domains to Sema-1a. This is in line with previous observations showing, with respect to GEF regulation, that protein-protein interactions and posttranslational modifications can result in the relief of auto-inhibitory intramolecular interactions, GEF relocalization, or downregulation of GEF activity (Schmidt and Hall, 2002).

The mammalian *p190* protein is required for axon guidance and fasciculation, and its function is regulated by phosphorylation events downstream of cell adhesion molecules (Brouns et al., 2001). Similarly, in fly mushroom body neurons, *p190* and cell adhesion/signaling molecules including integrins control axon branch stability (Billuart et al., 2001). We find here that *p190* knockdown leads to analogous defects in motor axon pathfinding and fasciculation, further supporting an evolutionarily conserved role for this GAP during neural development. Based upon the strong genetic interactions we observe between *p190* and *Sema-1a*, and also the increased defasciculation phenotypes in *p190* knockdown embryos, we propose that *p190* negatively regulates Sema-1a repulsive signaling. In addition, the antagonistic genetic interactions we observe between *p190* and *pbl* suggest that they compete to control Sema-1a reverse signaling. This competition could serve to rapidly amplify or inhibit Sema-1a-mediated signaling. Interestingly, we also observed synergistic interactions between *p190* and *pbl*, suggesting employment of a cyclic mode of action for Rho GTPase activation and inactivation in axon guidance (Luo, 2000). These distinct and cooperative functions may contribute to selective activation of Sema-1a repulsive signaling at different choice points. Taken together, our results support a model whereby Pbl and p190 together act to integrate target recognition and repulsive signaling resulting from reverse Sema-1a signal transduction events (Figure 8).

Semaphorin-1a Forward and Reverse Signaling

Sema-1a was initially identified as an axonal repellent that functions as a ligand for *PlexA* (Yu et al., 1998; Winberg et al., 1998). This Sema-1a ligand function is strongly supported by genetic analyses that define roles for Sema-1a-PlexA forward signaling in PNS motor axon pathfinding (Winberg et al., 1998; this present study). However, differences in *Sema-1a* and *PlexA* null mutant phenotypes, and also the lack of genetic interactions between

these mutants with respect to CNS defects, suggest that Sema-1a plays a unique role independent of PlexA in CNS axon guidance (Figures S8B–S8E). Here, we provide cellular and genetic evidence that Sema-1a forward signaling is largely responsible for Sema-1a-mediated CNS axon guidance, whereas both forward and reverse signaling are required for Sema-1a-mediated PNS motor axon pathfinding. In addition, Sema-1a reverse signaling is dependent upon opposing Pbl and p190 functions (Figure 8).

Sema-1a is highly expressed on embryonic motor and CNS axons and plays an important role in both CNS and PNS axon guidance (Yu et al., 1998). The neuronal requirement for Sema-1a in these guidance events fits well with our finding that the Sema-1a receptor function required for PNS axon guidance is controlled by neuronal Pbl and p190. Our genetic interaction analyses, however, suggest that PlexA does not function as a major Sema-1a ligand in both the embryonic PNS and the CNS, consistent with previous observations in the olfactory system (Sweeney et al., 2011), but, rather, cooperates with Sema-1a reverse signaling to mediate repulsion (Figure 8). Given that plexins harbor a GAP activity directed toward Ras GTPases (Oinuma et al., 2004; Yang and Terman, 2012), Sema-1a reverse signaling and the receptor function of PlexA likely converge on Rho and Ras GTPases, respectively, and these two small GTPases likely collaborate to control axonal defasciculation. Recent work suggests that Rap, not Ras, GTPases are the target of the PlexA GAP domain (Wang et al., 2012), and future work will determine which GTPases in vivo are regulated by plexin GAP activity.

Rho1 GTPases in Motor Axon Guidance

The Rho family of small GTPases, which includes *Rho*, *Rac*, and *Cdc42*, controls growth cone behavior through the regulation of actin dynamics (Hall and Lalli, 2010). In *Drosophila* neuromuscular development, overexpression of a dominant-negative (DN) Cdc42 causes motor neuron growth cone arrest. However, expression of DN Rac1 frequently results in parallel bypass phenotypes, indicative of defects in target recognition and axonal defasciculation (Kaufmann et al., 1998). Here, we observe that *Rho1* plays a critical role in Sema-1a-mediated motor axon repulsion, and that its activity is modulated by opposing Pbl and p190 functions specified by Sema-1a-mediated repulsive, and most likely attractive, signals (Figure S6). We also observed highly penetrant motor axon pathfinding defects in *Sema-1a*, *pbl*, and *p190* loss-of-function mutants (85%, 98%, and 66% of mutant hemisegments respectively). Furthermore, our finding that Sema-1a and Pbl collaborate to reduce cell size in cultured cells, and that this synergistic effect is reversed by inhibition of *Rho1* activity, support an essential role for *Rho1* in repulsive guidance at specific choice points. Previous studies show that *pbl* null alleles including pbl^2, pbl^3, and pbl^5, which we find here show strong genetic interactions with *Sema-1a*, strongly suppress the *Rho1*-induced rough eye phenotypes in *Drosophila*, and that Pbl interacts with Rho1, but not with Rac1 or Cdc42, in yeast two-hybrid assays (Prokopenko et al., 1999). Taken together, these observations strongly suggest that Sema-1a regulates the GEF activity of Pbl directed toward the Rho1 GTPase. Phenotypic analysis of *pbl* and *p190* mutants demonstrates an additional role for *Rho1* in regulating axon target recognition. In summary, our results suggest that Sema-1a-mediated reverse signaling pathways converge on Rho1 to control motor axon target recognition and guidance. It will be important to determine whether other transmembrane guidance cues best known as ligands, including vertebrate transmembrane semaphorins, also mediate receptor functions through direct modulation of Rho GTPase activities.

EXPERIMENTAL PROCEDURES

Drosophila Strains and Phenotypic Characterization

We used the w^{1118} strain as a wild-type control. The following flies were obtained from the Bloomington Stock Center: pbl^2, pbl^3, pbl^5, $pbl^{KG07669}$, pbl^{09645}, *UAS-pbl RNAi[t28343]*, *UAS-p190 RNAi[8.2]*, *UAS-p190 RNAi[5.2]*, *UAS-mycp190*, *e16E-GAL4*, and $Rho1^{72F}$. *UAS-pbl RNAi[v35349]* and *UAS-pbl RNAi[v35350]* were obtained from the Vienna *Drosophila* RNAi Center. All other strains were described previously: $Sema\text{-}1a^{PI}$ and *UAS-Sema-1a* (Yu et al., 1998); $PlexA^{Df(4)C3}$ (Winberg et al., 1998); $PlexB^{KG00878}$ (Ayoob et al., 2006); *Elav(2)-GAL4*, *Elav(3E)-GAL4*, and *24B-GAL4* (Luo et al., 1994); *Sca-GAL4* (Klaes et al., 1994); $GMR37C03^{GAL4}$ and $GMR37D12^{GAL4}$ (Pfeiffer et al., 2008). $p190^2$ was obtained from J. Cho. Phenotypic analyses of axon guidance defects were performed as described previously (Yu et al., 1998).

Expression Constructs and Mutagenesis

PlexB, Sema-1a, and Otk (LP17455) open reading frames (ORF) from cDNAs or EST clones were myc-tagged C-terminally and subcloned into pUAST (Brand and Perrimon, 1993). The UAS-PlexA-5xmyc was described previously (Wu et al., 2011). Pbl (SD01796), NTD[Pbl], CTD[Pbl], and p190 (RE10888) were HA-tagged N-terminally and similarly subcloned into pUAST. The UAS-CD8-EGFP (pUAST-DEST16) was obtained from the *Drosophila* Genomics Resource Center (DGRC). Serially deleted or point mutation constructs of Sema-1a ICD were generated using pUAST as represented in Figure 1C. All constructs for transgenic flies shown in Figure 6A were generated by polymerase chain reaction (PCR) and/or restriction enzyme-based strategies and inserted into a customized version of pUAST (pUAST-attB), which allows site-specific integration into predetermined landing sites (Bischof et al., 2007). To minimize position effects, all transgenic flies were generated using the same landing site (Strain 9750, BestGene). Integration and orientation were confirmed by a PCR-based assay with attP-F and attB-R primers (Venken et al., 2006).

Cell Contraction Assay in ML-DmBG2-c2 Cells

ML-DmBG2-c2 cells were maintained according to standard procedures (available at http://www.flyrnai.org/DRSC-PRC.html). Immunofluorescence microscopy and RNAi experiments were performed as described previously (Rogers and Rogers, 2008) but with a few modifications. Cells were fixed with 3.7% paraformaldehyde in PHEM buffer (60 mM PIPES, 25 mM HEPES, pH 7.0, 10 mM EGTA, 4 mM $MgSO_4$) for 10 min at room temperature. To knock down endogenous Rho1, 10 μg of dsRNA directed against Rho1 was first added to each well 30 min after transfection. After 2.75 days, another 10 μg of dsRNA was added to each well. By quantitative immunoblotting, we verified that *Rho1* dsRNA reduced endogenous protein levels by ~70% as compared to control cells (data not shown). More than 28 single, isolated, cells for each transfection experiment were analyzed for cell area using ImageJ. Primary antibodies used in this experiment were as follows: HA (3F10, Roche), myc (9E10, Sigma), GFP (rabbit and 3E6, Invitrogen), and Sema-1a (Yu et al., 1998) antibodies.

SUPPLEMENTAL INFORMATION

Supplemental Information includes eight figures and Supplemental Experimental Procedures and can be found with this article online at http://dx.doi.org/10.1016/j.neuron.2012.09.018.

ACKNOWLEDGMENTS

We thank Liqun Luo and Zhuhao Wu for comments on the manuscript; Kolodkin laboratory members for helpful discussions throughout this work; Joong Cho, the Bloomington Drosophila Stock Center, and Vienna Drosophila RNAi Center for strains; and the Drosophila Genomics Resource Center for clones and vectors. This work was supported by NIH R01 NS35165 (A.L.K.). A.L.K. is an Investigator of the Howard Hughes Medical Institute.

Accepted: September 11, 2012
Published: November 21, 2012

REFERENCES

Ayoob, J.C., Terman, J.R., and Kolodkin, A.L. (2006). *Drosophila* Plexin B is a Sema-2a receptor required for axon guidance. Development *133*, 2125–2135.

Bashaw, G.J., and Klein, R. (2010). Signaling from axon guidance receptors. Cold Spring Harb. Perspect. Biol. *2*, a001941.

Bellen, H.J., Levis, R.W., Liao, G., He, Y., Carlson, J.W., Tsang, G., Evans-Holm, M., Hiesinger, P.R., Schulze, K.L., Rubin, G.M., et al. (2004). The BDGP gene disruption project: single transposon insertions associated with 40% of Drosophila genes. Genetics *167*, 761–781.

Bellen, H.J., Levis, R.W., He, Y., Carlson, J.W., Evans-Holm, M., Bae, E., Kim, J., Metaxakis, A., Savakis, C., Schulze, K.L., et al. (2011). The *Drosophila* gene disruption project: progress using transposons with distinctive site specificities. Genetics *188*, 731–743.

Billuart, P., Winter, C.G., Maresh, A., Zhao, X., and Luo, L. (2001). Regulating axon branch stability: the role of p190 RhoGAP in repressing a retraction signaling pathway. Cell *107*, 195–207.

Bischof, J., Maeda, R.K., Hediger, M., Karch, F., and Basler, K. (2007). An optimized transgenesis system for *Drosophila* using germ-line-specific phiC31 integrases. Proc. Natl. Acad. Sci. USA *104*, 3312–3317.

Brand, A.H., and Perrimon, N. (1993). Targeted gene expression as a means of altering cell fates and generating dominant phenotypes. Development *118*, 401–415.

Brouns, M.R., Matheson, S.F., and Settleman, J. (2001). p190 RhoGAP is the principal Src substrate in brain and regulates axon outgrowth, guidance and fasciculation. Nat. Cell Biol. *3*, 361–367.

Cafferty, P., Yu, L., Long, H., and Rao, Y. (2006). Semaphorin-1a functions as a guidance receptor in the *Drosophila* visual system. J. Neurosci. *26*, 3999–4003.

Dent, E.W., Gupton, S.L., and Gertler, F.B. (2011). The growth cone cytoskeleton in axon outgrowth and guidance. Cold Spring Harb. Perspect. Biol. *3*, a001800.

Derijck, A.A., Van Erp, S., and Pasterkamp, R.J. (2010). Semaphorin signaling: molecular switches at the midline. Trends Cell Biol. *20*, 568–576.

Dickson, B.J. (2001). Rho GTPases in growth cone guidance. Curr. Opin. Neurobiol. *11*, 103–110.

Dickson, B.J. (2002). Molecular mechanisms of axon guidance. Science *298*, 1959–1964.

Egea, J., and Klein, R. (2007). Bidirectional Eph-ephrin signaling during axon guidance. Trends Cell Biol. *17*, 230–238.

Godenschwege, T.A., Hu, H., Shan-Crofts, X., Goodman, C.S., and Murphey, R.K. (2002). Bi-directional signaling by Semaphorin 1a during central synapse formation in *Drosophila*. Nat. Neurosci. *5*, 1294–1301.

Govek, E.E., Newey, S.E., and Van Aelst, L. (2005). The role of the Rho GTPases in neuronal development. Genes Dev. *19*, 1–49.

Hall, A., and Lalli, G. (2010). Rho and Ras GTPases in axon growth, guidance, and branching. Cold Spring Harb. Perspect. Biol. *2*, a001818.

Janssen, B.J., Robinson, R.A., Pérez-Brangulí, F., Bell, C.H., Mitchell, K.J., Siebold, C., and Jones, E.Y. (2010). Structural basis of semaphorin-plexin signalling. Nature *467*, 1118–1122.

Kaufmann, N., Wills, Z.P., and Van Vactor, D. (1998). *Drosophila* Rac1 controls motor axon guidance. Development *125*, 453–461.

Keshishian, H., Broadie, K., Chiba, A., and Bate, M. (1996). The *Drosophila* neuromuscular junction: a model system for studying synaptic development and function. Annu. Rev. Neurosci. *19*, 545–575.

Kim, J.E., Billadeau, D.D., and Chen, J. (2005). The tandem BRCT domains of Ect2 are required for both negative and positive regulation of Ect2 in cytokinesis. J. Biol. Chem. *280*, 5733–5739.

Klaes, A., Menne, T., Stollewerk, A., Scholz, H., and Klämbt, C. (1994). The ETS transcription factors encoded by the Drosophila gene *pointed* direct glial cell differentiation in the embryonic CNS. Cell *78*, 149–160.

Kolodkin, A.L., and Tessier-Lavigne, M. (2011). Mechanisms and molecules of neuronal wiring: a primer. Cold Spring Harb. Perspect. Biol. *3*, a001727.

Komiyama, T., Sweeney, L.B., Schuldiner, O., Garcia, K.C., and Luo, L. (2007). Graded expression of semaphorin-1a cell-autonomously directs dendritic targeting of olfactory projection neurons. Cell *128*, 399–410.

Landgraf, M., Bossing, T., Technau, G.M., and Bate, M. (1997). The origin, location, and projections of the embryonic abdominal motorneurons of *Drosophila*. J. Neurosci. *17*, 9642–9655.

Liu, H., Juo, Z.S., Shim, A.H., Focia, P.J., Chen, X., Garcia, K.C., and He, X. (2010). Structural basis of semaphorin-plexin recognition and viral mimicry from Sema7A and A39R complexes with PlexinC1. Cell *142*, 749–761.

Liu, X., Wang, H., Eberstadt, M., Schnuchel, A., Olejniczak, E.T., Meadows, R.P., Schkeryantz, J.M., Janowick, D.A., Harlan, J.E., Harris, E.A., et al. (1998). NMR structure and mutagenesis of the N-terminal Dbl homology domain of the nucleotide exchange factor Trio. Cell *95*, 269–277.

Luo, L. (2000). Rho GTPases in neuronal morphogenesis. Nat. Rev. Neurosci. *1*, 173–180.

Luo, L., Liao, Y.J., Jan, L.Y., and Jan, Y.N. (1994). Distinct morphogenetic functions of similar small GTPases: *Drosophila* Drac1 is involved in axonal outgrowth and myoblast fusion. Genes Dev. *8*, 1787–1802.

Mann, F., Chauvet, S., and Rougon, G. (2007). Semaphorins in development and adult brain: Implication for neurological diseases. Prog. Neurobiol. *82*, 57–79.

Nogi, T., Yasui, N., Mihara, E., Matsunaga, Y., Noda, M., Yamashita, N., Toyofuku, T., Uchiyama, S., Goshima, Y., Kumanogoh, A., and Takagi, J. (2010). Structural basis for semaphorin signalling through the plexin receptor. Nature *467*, 1123–1127.

Oinuma, I., Ishikawa, Y., Katoh, H., and Negishi, M. (2004). The Semaphorin 4D receptor Plexin-B1 is a GTPase activating protein for R-Ras. Science *305*, 862–865.

O'Keefe, D.D., Thor, S., and Thomas, J.B. (1998). Function and specificity of LIM domains in *Drosophila* nervous system and wing development. Development *125*, 3915–3923.

Pfeiffer, B.D., Jenett, A., Hammonds, A.S., Ngo, T.T., Misra, S., Murphy, C., Scully, A., Carlson, J.W., Wan, K.H., Laverty, T.R., et al. (2008). Tools for neuroanatomy and neurogenetics in *Drosophila*. Proc. Natl. Acad. Sci. USA *105*, 9715–9720.

Prokopenko, S.N., Brumby, A., O'Keefe, L., Prior, L., He, Y., Saint, R., and Bellen, H.J. (1999). A putative exchange factor for Rho1 GTPase is required for initiation of cytokinesis in *Drosophila*. Genes Dev. *13*, 2301–2314.

Prokopenko, S.N., He, Y., Lu, Y., and Bellen, H.J. (2000). Mutations affecting the development of the peripheral nervous system in Drosophila: a molecular screen for novel proteins. Genetics *156*, 1691–1715.

Rogers, S.L., and Rogers, G.C. (2008). Culture of *Drosophila* S2 cells and their use for RNAi-mediated loss-of-function studies and immunofluorescence microscopy. Nat. Protoc. *3*, 606–611.

Saito, S., Liu, X.F., Kamijo, K., Raziuddin, R., Tatsumoto, T., Okamoto, I., Chen, X., Lee, C.C., Lorenzi, M.V., Ohara, N., and Miki, T. (2004). Deregulation and mislocalization of the cytokinesis regulator ECT2 activate the Rho signaling pathways leading to malignant transformation. J. Biol. Chem. *279*, 7169–7179.

Schmidt, A., and Hall, A. (2002). Guanine nucleotide exchange factors for Rho GTPases: turning on the switch. Genes Dev. *16*, 1587–1609.

Shen, K., and Cowan, C.W. (2010). Guidance molecules in synapse formation and plasticity. Cold Spring Harb. Perspect. Biol. *2*, a001842.

Sweeney, L.B., Chou, Y.H., Wu, Z., Joo, W., Komiyama, T., Potter, C.J., Kolodkin, A.L., Garcia, K.C., and Luo, L. (2011). Secreted semaphorins from degenerating larval ORN axons direct adult projection neuron dendrite targeting. Neuron *72*, 734–747.

Symons, M., and Settleman, J. (2000). Rho family GTPases: more than simple switches. Trends Cell Biol. *10*, 415–419.

Toyofuku, T., Zhang, H., Kumanogoh, A., Takegahara, N., Yabuki, M., Harada, K., Hori, M., and Kikutani, H. (2004). Guidance of myocardial patterning in cardiac development by Sema6D reverse signalling. Nat. Cell Biol. *6*, 1204–1211.

Ui, K., Nishihara, S., Sakuma, M., Togashi, S., Ueda, R., Miyata, Y., and Miyake, T. (1994). Newly established cell lines from *Drosophila* larval CNS express neural specific characteristics. In Vitro Cell. Dev. Biol. Anim. *30A*, 209–216.

Van Vactor, D., Sink, H., Fambrough, D., Tsoo, R., and Goodman, C.S. (1993). Genes that control neuromuscular specificity in Drosophila. Cell *73*, 1137–1153.

Venken, K.J., He, Y., Hoskins, R.A., and Bellen, H.J. (2006). P[acman]: a BAC transgenic platform for targeted insertion of large DNA fragments in *D. melanogaster*. Science *314*, 1747–1751.

Wang, Y., He, H., Srivastava, N., Vikarunnessa, S., Chen, Y.B., Jiang, J., Cowan, C.W., and Zhang, X. (2012). Plexins are GTPase-activating proteins for Rap and are activated by induced dimerization. Sci. Signal. *5*, ra6.

Winberg, M.L., Noordermeer, J.N., Tamagnone, L., Comoglio, P.M., Spriggs, M.K., Tessier-Lavigne, M., and Goodman, C.S. (1998). Plexin A is a neuronal semaphorin receptor that controls axon guidance. Cell *95*, 903–916.

Wu, Z., Sweeney, L.B., Ayoob, J.C., Chak, K., Andreone, B.J., Ohyama, T., Kerr, R., Luo, L., Zlatic, M., and Kolodkin, A.L. (2011). A combinatorial semaphorin code instructs the initial steps of sensory circuit assembly in the Drosophila CNS. Neuron *70*, 281–298.

Yang, T., and Terman, J.R. (2012). 14-3-3ε couples protein kinase A to semaphorin signaling and silences plexin RasGAP-mediated axonal repulsion. Neuron *74*, 108–121.

Yu, H.H., Araj, H.H., Ralls, S.A., and Kolodkin, A.L. (1998). The transmembrane Semaphorin Sema I is required in *Drosophila* for embryonic motor and CNS axon guidance. Neuron *20*, 207–220.

Yu, L., Zhou, Y., Cheng, S., and Rao, Y. (2010). Plexin a-semaphorin-1a reverse signaling regulates photoreceptor axon guidance in *Drosophila*. J. Neurosci. *30*, 12151–12156.